HOSTED BY

ELSEVIER

Available online at www.sciencedirect.com

ScienceDirect

Soils and Foundations xxx (2018) xxx–xxx

SOILS AND FOUNDATIONS

www.elsevier.com/locate/sandf

Comprehensive group pile settlement formula based on 3D finite element analyses

Murat Hamderi

Faculty of Engineering, Turkish-German University, Istanbul, Turkey

Received 27 December 2016; received in revised form 8 July 2017; accepted 14 August 2017

Abstract

In the past, formulas for the settlement of group piles considered only a few input parameters and offered only a limited approximation of the actual settlement. Nowadays, however, thanks to the fast-growing performance of personal computers, it is possible to create large 3-dimensional finite element models with a better and more reliable settlement approximation. On the other hand, 3-dimensional finite element methods for piles are not very common in practice since the required procedure is comparatively cumbersome, expensive and needs a bit more expertise. In order to address this issue, a pile settlement formula was developed in the present study based on about 120 finite element model configurations. The group pile settlement formula incorporates the dimensions of a rectangular raft, namely, the diameter, length and spacing of the piles, vertical uniform pressure, soil moduli up to five layers, ultimate pile-soil resistance, pile-tip resistance and elastic modulus of the piles. In addition to this, the average deflection rate of the raft is estimated. The reliability of the finite element model is verified through laboratory-scale group pile tests. The proposed formula is also checked against five well-documented case studies. The formula may help engineers optimize group pile configurations more efficiently by applying the quality of the 3D finite element estimation to practice.

Keywords: Group pile formula; TNO DIANA; Settlement; PLAXIS 3D; Subgrade modulus

1. Introduction

The demand for pile foundations has increased with the fast development of tall and heavy structures in growing cities. As a result of this, accurate estimations of group pile settlements have become more important. In particular, strict foundation raft settlement or deflection rate requirements dictated by national codes have initiated the search for more sophisticated methods.

For the last 60 years, numerous approaches have been proposed for estimating the settlement of group piles. The leading approaches can be categorized as follows (Dung et al., 2010): (1) The empirical or semi-empirical approach (Meyerhof, 1976; Vesic, 1977), (2) The equivalent raft or pier approach (Terzaghi and Peck, 1967; Fellenius, 1991; Poulos, 1993; Yamashita et al., 2015), (3) The interaction factor approach (Poulos and Davis, 1980; Randolph and Wroth, 1979) and (4) The numerical analysis approach (Chow, 1986; Clancy and Randolph, 1996). The comparison and prediction capabilities of these methods have been well-documented in a study by Dung et al. (2010). Their study reports that the relative standard deviation in settlements calculated by the four different methods is in the range of 50%. Such a deviation in group pile settlements indicates a major problem with accuracy. Besides these methods, Shahin (2014) used recurrent neural networks calibrated with in-situ full-scale pile load tests to predict pile settlements.

Peer review under responsibility of The Japanese Geotechnical Society.

E-mail address: hamderi@tau.edu.tr

https://doi.org/10.1016/j.sandf.2017.11.012

There are various factors that can influence the settlement of group piles. One of them is the pile installation method. The effects of the pile installation method have been investigated by several researchers (Housel and Burkey, 1948; Cummings et al., 1950; Lambe and Hom, 1965; Lo and Stermac, 1965; Orrje and Broms, 1967; Hanna, 1967; Fellenius and Broms, 1969; Koizumi and Ito, 1967; D'Appolonia and Lambe, 1971; Fellenius, 1984, 2006). These studies were mostly targeted at solving problems such as the gain in bearing capacity or the loss due to pile driving (usually in clay), post-pile displacement due to negative skin friction and the development of pore pressure. In recent years, some researchers have developed rate-dependent models for soft soils which are helpful for modelling the effects of pile installation (Zhu and Yin, 2000; Grimstad et al., 2010; Sivasithamparam et al., 2013). Ottolini and Dijkstra (2014) reported that until that time there had been no efficient numerical model that considered the installation effects especially on the settlement of group piles. A recent study by Phuong et al. (2016) demonstrated that the installation of a single displacement pile could be modelled well with the material point simulation method (MPM). The numerical results reported in their study were verified by centrifuge tests. It has been reported that the MPM, in conjunction with the hypoplastic constitutive model (formulated by Von Wolffersdorff, 1996) makes it possible to model the large strains developing around a pile tip during pile driving. According to the study, the bearing capacity of a single pile increased about 2.5 times, while the void ratio around the pile tip decreased by about 5% (=compaction) after pile driving.

Nowadays, engineers are trying to enhance their settlement predictions by implementing 3-dimensional finite element (3D FE) models. On the other hand, this approach is not yet widely used in engineering practice since it is relatively cumbersome and expensive.

In order to address this issue, a group pile settlement formula was developed in this study based on about 120 finite element model configurations. The group pile settlement formula incorporates the dimensions of a rectangular raft, namely, diameter, length and spacing of the piles, vertical uniform pressure, soil moduli up to five layers, ultimate pile-soil resistance, pile tip resistance and elastic modulus of the piles. The reliability of the formula was checked against another 3D FE program (PLAXIS 3D) and also against five well-documented case studies.

2. Verification of finite element model with embedded beams

2.1. Finite element program

In this study, the TNO-DIANA finite element (FE) program is used to model the group piles. The main reason for using DIANA is its capability to model piles as embedded beam elements which have a nonlinear solid-beam slip surface (Diana User's Manual, Release 9.5). Embedded piles can be accommodated in solid elements relatively easily, because their nodes are not required to coincide with the nodes of the adjacent solid elements. A typical illustration of an embedded beam (embedded pile) is given in Fig. 1S (in the Supplementary Data file).

2.2. Setup of laboratory-size group pile test for verification

The verification test was performed in a 0.8 m × 0.8 m × 0.8 m MDF (Medium-Density-Fibreboard) box filled with dry sand (Fig. 1). The testing facility was used not only for the plate loading test, but also for the group pile loading test. The loading plate applied for the plate loading test was manufactured from a 0.4 m × 0.4 m × 0.02 m MDF piece. A similar size MDF plate was rigidly attached to 25 wooden piles and served as a small-size group pile foundation (Fig. 1). Each pile was 0.35 m in length and 0.02 m in diameter.

In each test, the required vertical weight was provided by an HDPE (High Density Polyethylene) cylindrical water tank located at the centre of the loading plate (Table 1 and Fig. 2). The distribution of the water pressure over the raft was expected to be quite uniform since the cylindrical water

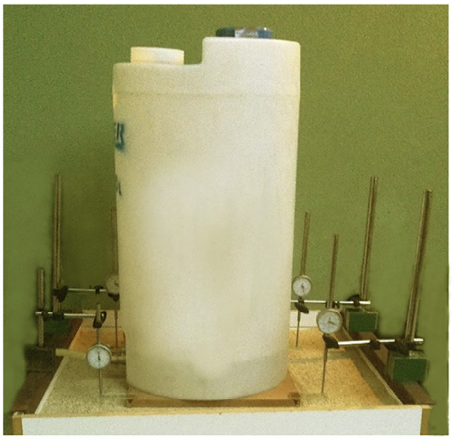

a) Plate loading test

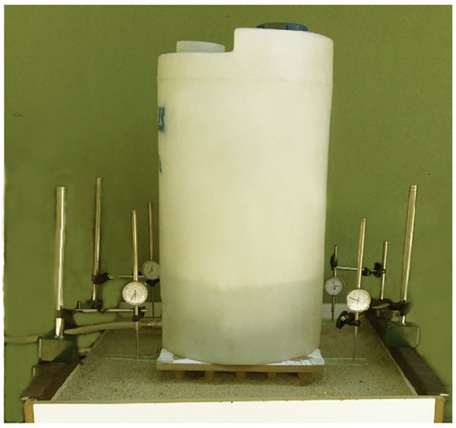

b) Group pile loading test

Fig. 1. (a) Plate loading test and (b) Group pile loading test.

Please cite this article in press as: Hamderi, M., Comprehensive group pile settlement formula based on 3D finite element analyses, Soils Found. (2018), https://doi.org/10.1016/j.sandf.2017.11.012

Table 1
List of verification tests and maximum load applied.

Plate loading			Group pile loading		
Test 1	Test 2	Test 3	Test 1	Test 2	Test 3
Max. load = 8.22 kPa over a circular area with 0.38 m diameter.					

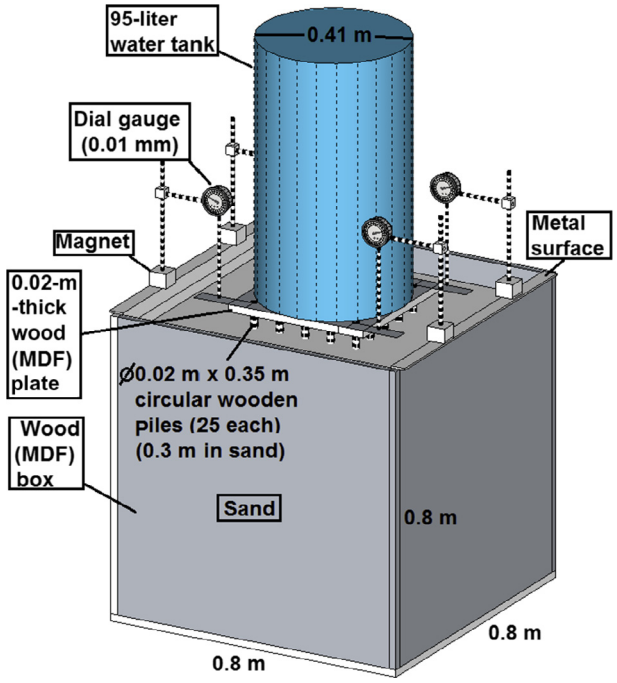

Fig. 2. Setup of laboratory-size group pile test.

tank had a flat and fairly flexible bottom. The settlement of the plate was measured with four dial gauges with an accuracy of 0.01 mm.

In each test, the density of the dry-pluviated sand was 1.38 g/cm^3. The pluviation was achieved by pouring sand through a meshed-plate affixed at the top of the sand box. This method was repeated before each test. The achieved density could easily be checked by measuring the height of the sand in the cubical-shaped box. The minimum and maximum densities of the sand were 1.34 g/cm^3 and 1.68 g/cm^3, respectively. The uniformity coefficients, $c_u = d_{60}/d_{10}$ and d_{50} (d_x = diameter for which x% of the sample passes) for the sand were 4.5 and 0.8 mm, respectively.

During the dry pluviation, the wooden pile-plate assembly rested inside the box. The pluviated sand mostly filled up the spaces between the piles by flowing through them. However, before the completion of the sand pluviation, there were some spaces left between the piles where the sand level came out a bit low. The uneven sand level between the piles was adjusted gently by a small ruler. In the end, small gaps were left between the plate and the sand.

2.3. Setup of finite element model used for verification

Two similar finite element models were created for the plate loading and the group pile loading tests, respectively. These models are illustrated in Fig. 3. The main difference between the two models was basically the foundation type. For the plate loading model, the foundation plate which was in direct contact with the sand, was meshed with trihedral solid elements. In contrast to the plate loading model, the pile raft in the group pile model had no direct contact with the sand; rather, it had contact through the piles (Fig. 3).

The maximum total weight applied was about 0.93 kN (8.22 kPa over a circular area with a diameter of 0.38 m). The parameters used for the verification model are given in Table 2. The modulus of elasticity values for the MDF specimens and the beech wood piles were estimated through strain gauge measurements on specimens which were loaded with block weights. Strain gauge readings were taken from two opposite sides of each beach wood pile or MDF specimen. Later, they were averaged and rounded out. The friction angle of the sand was determined by direct shear tests (ASTM D3080). A typical density value of 0.8

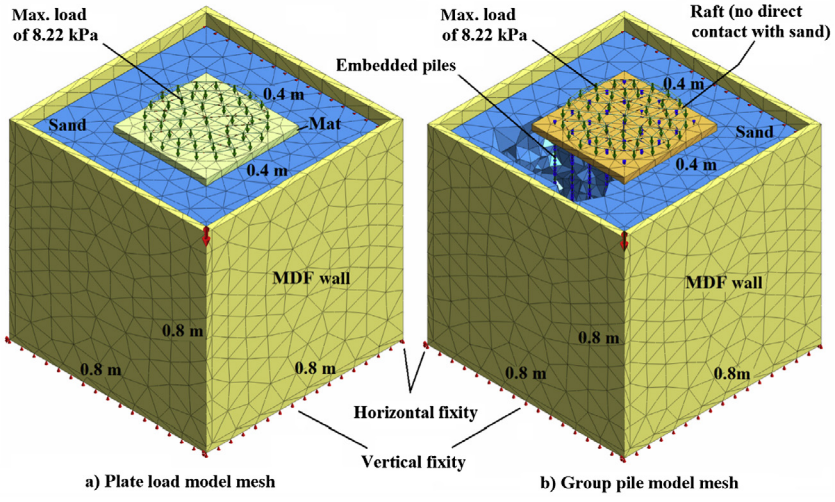

Fig. 3. Mesh of (a) Plate loading model and (b) Group pile loading model.

Please cite this article in press as: Hamderi, M., Comprehensive group pile settlement formula based on 3D finite element analyses, Soils Found. (2018), https://doi.org/10.1016/j.sandf.2017.11.012

Table 2
Parameters of finite element model for verification.

Material	Elem. Type	Mat. Model	Density (g/cm^3)	Frict. Angle (^{o})	Cohe. (kPa)	Mod. of Elast. (MPa)	Ult. Slide Resist. (kN/m)	Ult.Tip Resist. (kN)	Thick./ Dia. (m)	Poisson's Ratio
Sand	Solid	Mohr-Coulomb	1.38	32	0.5	5@top 20@bottom	–	–	–	0.35
MDF	Solid	Linear elastic	0.8	–	–	4000	–	–	0.02	0.3
Beech-wood piles	Beam with interface	Elastic beam with interface	0.8	–	–	5000	0.2	0.1	0.02	0.3

g/cm^3 was assigned to the wood piles and MDF specimens from the table provided in the book by Domone and Illston (2010). The density of the sand could easily be calculated by measuring the weight and the volume of the sand placed into the cube-shaped box. A typical Poisson's ratio of 0.3 was assigned to the wood piles and the MDF specimens (Domone and Illston, 2010).

2.4. Steps of verification

The verification was performed in a controlled manner, which was accomplished by changing only one condition between the two tests. This condition was basically the foundation type; it was changed from raft to pile-raft. Following this method allowed the isolation of the estimation errors in the parameters such as the modulus of elasticity. The steps of the verification are schematized in Fig. 4.

In Fig. 5, the displacement-pressure plots of three plate loading tests are compared with one obtained through the FE simulation. According to Fig. 5, in the early moments of the physical tests, the displacement increases at a higher rate than the one observed in the FE model. The main reason behind this is that the confining pressure underneath the plate is very low and, as a result, the soil becomes more vulnerable to local mini failures due to the insufficient shear strength especially along the edges. Interestingly, this trend does not repeat in the pressure-settlement curves of the pile load test demonstrated in Fig. 6. In this case, the pressure-displacement curve has more of a traditional appearance. An elastic zone appears between the displacement values

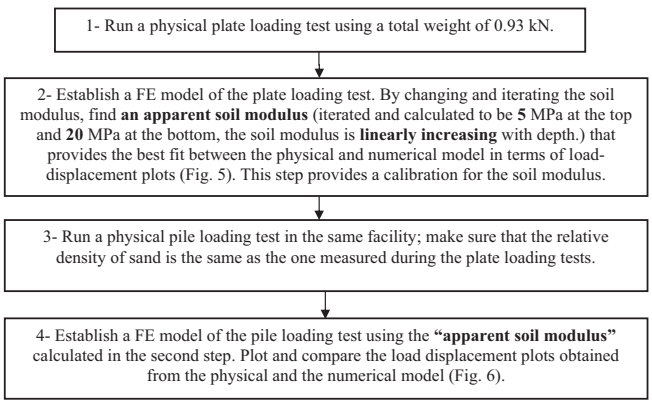

Fig. 4. Verification steps of model.

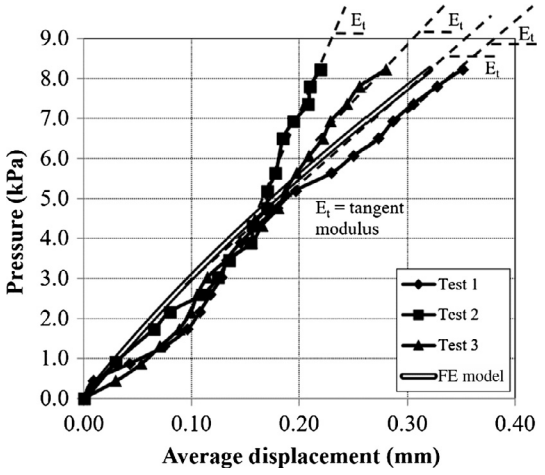

Fig. 5. Settlement observed during three physical plate loading tests (average of four measurements on sides) and their FE model with apparent soil modulus of 5–20 MPa.

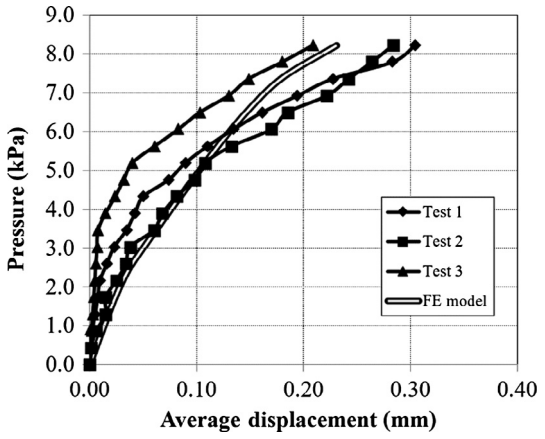

Fig. 6. Settlement observed during three physical group pile loading tests (average of four measurements on sides) and their FE estimation.

of 0 and 0.025 mm; and subsequently, plastic deformation begins. At the early stages, the FE model-based pressure-displacement curve is quite similar to the one obtained from Test 2. Overall, the plot demonstrates a fairly good match between the simulated and the measured test results. It should be mentioned here that the test and the simulation results would have matched much better if our sand had been denser, because dense sand would have behaved more elastically and experienced fewer plastic deformations

Please cite this article in press as: Hamderi, M., Comprehensive group pile settlement formula based on 3D finite element analyses, Soils Found. (2018), https://doi.org/10.1016/j.sandf.2017.11.012

Table 3
Range of input parameters incorporated in FE models for the formula derivation.

No	Description	Sym.	Range/Values	Unit	No	Description	Sym.	Range/Values	Unit
1	Spacing of piles @ x direction	s_{px}	(1–6), 1, 1.5, 2, 2.5, 3, 3.5, 5, 6	Mm	8	Soil modulus around piles	E_1, E_2, E_3 E_4	(10–300), 10, 20, 25, 29, 30, 32, 32.5, 33, 34, 35, 36, 38, 40, 43, 47.5, 50, 55, 60, 75, 85, 100, 104, 300	MPa
2	Spacing of piles @ y direction	s_{py}	(1–6), 1, 1.5, 2, 2.5, 3, 3.5, 5, 6	m	9	Soil modulus below piles	E_5	(10–300), 10, 20, 25, 30, 34, 35, 40, 50, 60, 75, 80, 85, 100, 180, 300	MPa
3	Length of piles	le	(5–40), 5, 7, 8, 10, 11, 12, 14, 15, 16, 20, 30, 40	m	10	Distributed vertical load	ld	(100–800), 100, 200, 250, 300, 350, 360, 400, 450, 500, 750, 800	kPa
4	Diameter of piles	di	(0.25–2) ,0.25, 0.4, 0.5, 0.65, 0.8, 1, 2	m	11	Ult. pile-soil friction	fr	(150–500), 150, 175, 200, 225, 300, 350, 400, 500	kN/m
5	Width of raft @ x direction	wi_x	(10–50), 10, 20, 35, 40, 45, 50	m	12	Ult. tip resistance	tr	(50–10,000), 50, 100, 500, 1000, 2000, 5000, 10,000	kN
6	Width of raft @ y direction	wi_y	(10–50), 10, 20, 25, 35, 40, 50	m	13	Pile tip to bedrock distance	bed	(30–100), 30, 34, 35, 36, 38, 39, 40, 42, 43, 45, 50, 60, 70, 90, 100	m
7	Elastic mod. of pile conc.	E_c	(10–50), 10, 25, 40, 50	GPa	14	Raft thickness	th	(0.5–2.5), 0.5, 1, 1.5, 2.5	m

under the same load. However, we preferred loose sand because it was easier to adjust its relative density and place it uniformly between the piles (no compaction was needed). In the verification tests, the average soil modulus of the sand was 12.5 MPa (5 MPa at the top and 20 MPa at the bottom); the soil modulus increased linearly with depth. During the pile formula derivation, we avoided using soil modulus values smaller than 10 MPa, due to the fact that we observed highly plastic behaviour below this value (see rows 7 and 8 in Table 3). Overall, the results demonstrate that the FE program DIANA can be a good tool for the settlement formula derivation.

3. Details of formula derivation

The settlement formula derivation includes five steps. They are: (1) Creation of a database composed of settlement values which are produced from 120 FE model configurations that were run with different parameter settings, (2) Estimation of the formula coefficients by a regression analysis, (3) Performance check of the formula using eight additional model configurations created in another finite element program called "PLAXIS 3D", (4) Performance check of the formula using five case histories reporting the measured settlements of group piles and (5) Comparison of the offered formula with another well-established group pile settlement formula.

3.1. Creation of settlement database from finite element models

A settlement formula with high estimation capabilities required about 120 FE model configurations. The varying model parameters were basically the width (wi_x), length (wi_y) and thickness (th) of the rectangular raft, the diameter (di), length (le) and spacing of the piles (sp_x and sp_y), the applied uniform load (ld), the soil moduli up to five layers (E_1, E_2, E_3, E_4 and E_5), the ultimate pile-soil friction (fr), the pile tip resistance (tr) and the elastic modulus of concrete (E_c). The range of parameters that were incorporated in the finite element model is given in Table 3. This table also demonstrates the formula's best applicability range. Beyond this range, the formula is still valid; however, it may not be as accurate as stated in Sections 3.3 and 3.4. For example, for a pile-raft system with the following parameters, wix = wiy = 20 m, th = 1 m, di = 0.5 m, le = 15 m, spx = spy = 2 m, ld = 250 kPa, E_1= E_2 = E_3 = E_4 = 25,000 kPa, E_5 = 50,000 kPa, fr = 300 kN/m, tr = 500 kN and E_c = 20,000 MPa, the settlement of the system can be calculated quite well because the magnitudes of all the parameters fall into the range given in Table 3. On the other hand, for example, if the settlement is calculated in a poor alluvial soil having a soil modulus of 2000 kPa (unlike the one above, E_{1-4} = 25,000 kPa), the formula may produce less accurate results because the modulus of the system under focus is much smaller than the minimum soil modulus used in the source FE models (min. E_{1-4} = 10,000 kPa, Table 3). Some of the parameters that were fixed for all the finite element configurations are given in Table 4.

In the analyses, the Mohr-Coulomb (M-C) soil model was incorporated. A parametric study was conducted on the M-C strength parameters (friction angle and cohesion) in order to investigate how closely these parameters are related to the settlement. It was found that these parameters had no direct influence on the settlement behaviour. This is acceptable because a group pile settlement problem does not take place in the failure state in which the soil strength parameters play a particularly important role. In other words, the deformations of group pile systems more or less stay in the elastic range. As a result, implementing a more sophisticated constitutive model is not preferable.

The general geometrical configuration of a group pile finite element model is illustrated in Fig. 7.

Please cite this article in press as: Hamderi, M., Comprehensive group pile settlement formula based on 3D finite element analyses, Soils Found. (2018), https://doi.org/10.1016/j.sandf.2017.11.012

Table 4
Description of material input parameters incorporated in FE models.

Material	Elem. Type	Mat. Model	Density (g/cm^3)	Frict. Angle (°)	Cohe. (kPa)	Mod. of Elast. (GPa)	Poisson's Ratio
Soil	Solid	Mohr-Coulomb	1.7	32	0.5	Table 3	0.35
Raft concrete	Solid	Linear- elastic	2.4	–	–	25	0.2
Pile concrete	Solid	Linear- elastic	2.4	–	–	10–50	0.2

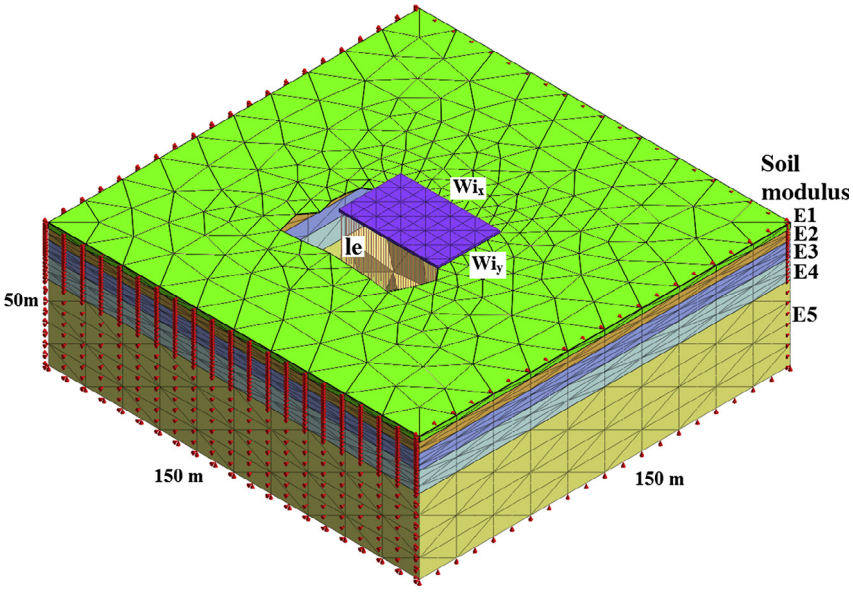

Fig. 7. Example mesh of model with 25 m × 40 m raft.

The details of the rectangular pile-raft system are given in Fig. 8. It should be noted that the sum of the thicknesses of the first four layers is equal to the pile length. The order of the distribution of thicknesses around the piles is 1/10 le, 2/10 le, 3/10 le and 4/10 le from the top to the bottom direction (Fig. 8).

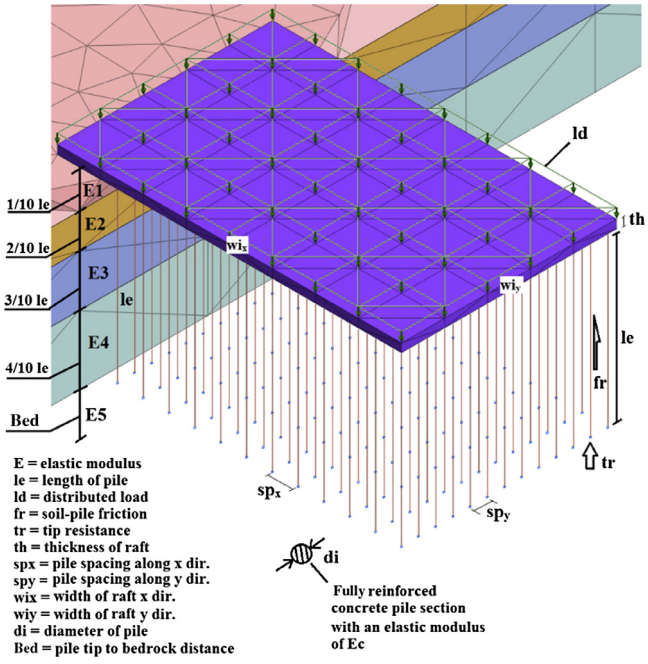

Fig. 8. Details of rectangular group pile foundation.

3.1.1. Output of finite element runs

A sample settlement output obtained from the program is shown in Fig. 9. The settlement values at the centre and at the corner of the raft were used as input for the derivation of the settlement formula.

3.2. Derivation of settlement formula

The settlement dataset obtained from the finite element runs include the values of the settlement at the centre and at the corner of the raft. The derived settlement formula is given as follows:

$$\text{Settlement} = S = S_b \cdot \left(\frac{sp_x.sp_y + u_1}{u_2}\right)^a \cdot \left(\frac{le}{u_3}\right)^b \cdot \left(\frac{di + u_4}{u_5}\right)^c \cdot \left(\frac{wi_x.wi_y}{u_6}\right)^d \cdot \left(\frac{0.1E_1 + 0.2E_2 + 0.3E_3 + 0.4E_4 + u_7}{u_8}\right)^e \cdot \left(\frac{E_5}{u_9}\right)^f \cdot \left(\frac{ld}{u_{10}}\right)^g \cdot \left(\frac{fr}{u_{11}}\right)^h \cdot \left(\frac{tr}{u_{12}}\right)^i \cdot \left(\frac{bed}{u_{13}}\right)^j \cdot \left(\frac{th}{u_{14}}\right)^k \cdot \left(\frac{Ec}{u_{15}}\right)^l \quad (1)$$

where S is the calculated settlement and "S_b" is the base settlement in meters, respectively. The symbols a, b, c, d, e, f, g, h, i, j, k and l are *unitless fitting coefficients* (see

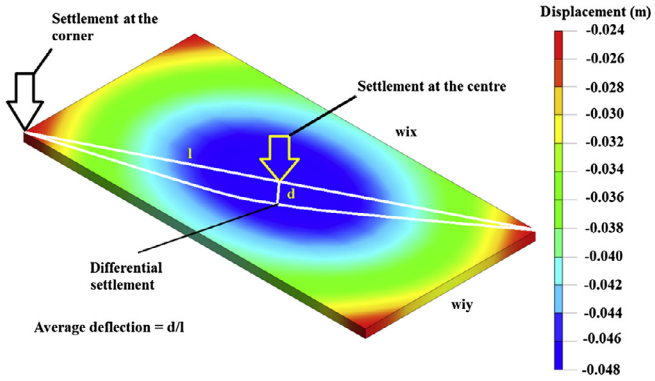

Fig. 9. Sample settlement output of 25 m × 40 m pile-raft foundation.

Table 5
Unitless fitting coefficients of settlement formula.

@centre	**a**	**b**	**c**	**d**	**e**	**f**
	0.1406	−0.2999	−0.2274	0.5286	−0.4275	−0.6229
	g	**h**	**i**	**j**	**k**	**l**
	1.1082	−0.1025	−0.0267	0.1903	−0.1582	−0.0537
@corner	**a**	**b**	**c**	**d**	**e**	**f**
	0.2037	−0.3371	0.1072	0.2898	−0.4558	−0.7406
	g	**h**	**i**	**j**	**k**	**l**
	1.0784	−0.1372	−0.0348	0.2060	0.0679	−0.0490

Table 6
Fitting constants of settlement formula (with units).

Constant	Constant value for S_{centre}	Constant value for S_{corner}	Unit
S_b	0.3287	3.7193	[m]
u_1, u_2, u_6	1	1	[m^2]
u_3, u_4, u_5	1	1	[m]
u_7	10,000	10,000	[kN/m^2]
u_8, u_9, u_{10}	1	1	[kN/m^2]
u_{11}	500	500	[kN/m]
u_{12}	1000	1000	[kN]
u_{13}, u_{14}	1	1	[m]
u_{15}	25,000	25,000	[MPa]

Table 5). The physical meaning of each coefficient is explained in Section 4. On the other hand, u_1, u_2 … u_{15} are *the fitting constants with units* (see Table 6). u_3, u_5, u_6, u_8, u_9, u_{10}, u_{13} and u_{14} were included only to establish dimension compatibility. On the other hand, the fitting constants, u_1, u_4 and u_7, are included in the terms in the $(\ldots + u_n)^n$ format to enhance the fitting (R^2) performance of the formula. Further details, including the derivation steps, are discussed in Supplementary Data S.3.2.

The formula is capable of calculating the settlement at the centre (S_{centre}) or at the corner (S_{corner}) of the raft depending on the fitting sets used (Tables 5 and 6).

The average deflection of the foundation can be calculated with the following formula:

$$Average\,Deflection = Def = \frac{(S_{centre} - S_{corner})}{\left(\left(\frac{wi_x}{2}\right)^2 + \left(\frac{wi_y}{2}\right)^2\right)^{0.5}} \quad (2)$$

The geometrical explanation of the deflection formula in illustrated in Fig. 9.

3.3. Performance check of formula against two geotechnical FE software packages

In this section, the proximity of the results offered by the settlement formula will be compared with that offered by TNO-DIANA in terms of the R^2 values. The related plots which are used to calculate the R^2 values are demonstrated in Fig. 10a and b. The y axes of the plots demonstrate the settlement values calculated through about 120 FE runs, whereas the x axes demonstrate the settlement results calculated through the proposed formula. The fitting performance of the formula is considerably high because the R^2 value in both situations is very close to 1 ($R^2 > 0.9950$) and the fitted linear equation is close to "y = x".

On the other hand, it is considered that it would be reasonable to check the performance of the settlement formula against an FE program which was not formerly used in the process of formula derivation. The best candidate was the geotechnical FE program, called PLAXIS 3D, which also accommodates embedded pile elements like TNO DIANA.

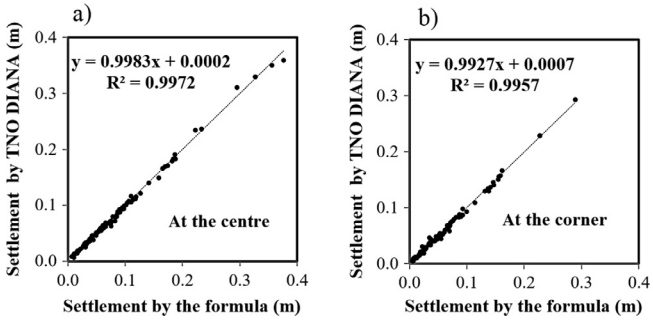

Fig. 10. Comparison of settlement results obtained through formula and TNO DIANA, (a) At the centre and (b) At the corner.

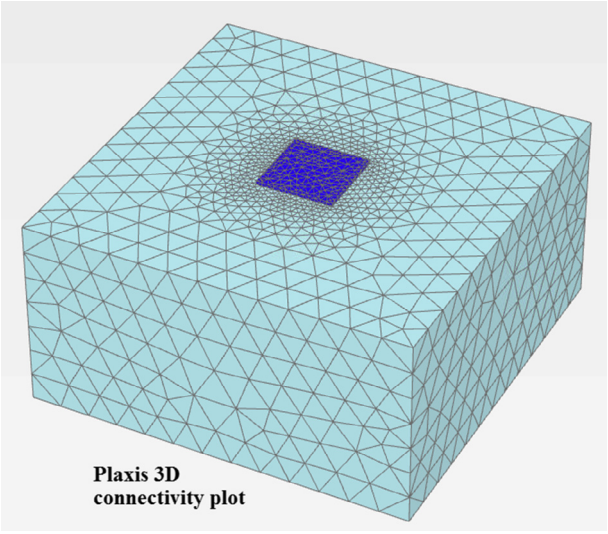

Fig. 11. PLAXIS 3D mesh.

Table 7
Parameters used to check performance of formula against PLAXIS 3D.

FE Code	No	fr (kN/m)	tr (kN)	sp_x (x)	sp_y (x)	le (m)	di (m)	wi_x (m)	wi_y (m)	Pile Tip to Bedrock Dist. (m)	th (m)
PLAXIS 3D	1	500	50	3	3	20	1	20	20	30	1
	2	500	50	3	3	20	1	20	20	30	1
	3	500	50	3	3	20	1	20	20	30	1
	4	500	50	3	3	20	1	20	20	30	1
	5	500	50	3	3	20	1	20	20	30	1
	6	500	50	3	3	10	1	40	40	30	1
	7	500	50	3	3	10	1	40	40	30	1
	8	500	50	3	3	10	1	40	40	30	1

FE Code	No	E_1 (kPa)	E_2 (kPa)	E_3 (kPa)	E_4 (kPa)	E_5 (kPa)	ld (kPa)	E_c (MPa)	Settl. FE Code (m)	Sett. Formula (m)	Diff.
PLAXIS 3D	1	10,000	10,000	10,000	10,000	10,000	200	25,000	**0.131**	**0.129**	**1.72%**
	2	20,000	20,000	20,000	20,000	20,000	200	25,000	**0.0689**	**0.070**	**2.03%**
	3	30,000	30,000	30,000	30,000	30,000	200	25,000	**0.047**	**0.048**	**2.74%**
	4	40,000	40,000	40,000	40,000	40,000	200	25,000	**0.036**	**0.037**	**1.92%**
	5	50,000	50,000	50,000	50,000	50,000	200	25,000	**0.03**	**0.030**	**1.54%**
	6	30,000	30,000	30,000	30,000	30,000	100	25,000	**0.0626**	**0.057**	**8.34%**
	7	40,000	40,000	40,000	40,000	40,000	100	25,000	**0.048**	**0.044**	**9.16%**
	8	50,000	50,000	50,000	50,000	50,000	100	25,000	**0.038**	**0.035**	**7.63%**
									Avg. Diff. →		**4.39%**

The FE model created in PLAXIS 3D (Plaxis 3D user's Manual, 2013) is very similar to the one created in TNO DIANA (Fig. 11). The model had fixed raft dimensions of 20 m × 20 m. Other parameters, such as the soil modulus, pile length and applied load, were changed to produce various configurations. The details and the results of this study are briefly summarized in Table 7.

The total maximum settlements calculated by the formula and PLAXIS 3D were only 4.39% different. The plots between the settlement results of the formula and PLAXIS 3D are demonstrated in Fig. 2S. Once again, the relation results had a considerably high R^2 value of 0.9937. This is one good example demonstrating that the results of the offered formula are consistent with those of another FE program which is widely used in geotechnical engineering.

3.4. Performance check of formula against case studies

In this section, the proposed pile settlement formula will be checked against five case studies in which the settlements were monitored for 3–10 years. During the first four case studies, the total amount of settlement increased proportionally with the building construction whereas, in the last case (Goossens and Van Impe, 1991), there was a considerable amount of post-settlement after the completion of the building.

The formula was able to estimate the settlements with considerable success, while the percent deviation between the predicted and the measured settlements at the centre was only 10.7%. The absolute deviation of the formula was relatively low for the first four cases (max. 10 mm) in which there was no or only a limited amount of consolidation behaviour. However, in the last case, the absolute deviation increased up to 34 mm. This was due to the fact that, quite a bit of post-settlement (due to consolidation) occurred in the last case. The formula also estimated the settlements at the corner of the raft fairly well. The percent deviation between the predicted and the measured settlements was 26.7%. The absolute deviation of the formula in calculating the corner settlement was relatively low (max. 8 mm) for the first four cases in which there was no or only a limited amount of consolidation behaviour. In the last case, the absolute deviation increased up to 57 mm. The details of these five case studies are given in Table 8. A comparison of the deflection was also made and the deviation was found to be 44.0%. A comparison of the data for the corner settlement and the deflection was not given for Case 4 since the settlement data near the corner were not reported in the related study.

3.4.1. Procedure for soil modulus estimation

The soil modulus was estimated based on the equations provided by Bowles (1997) and Budhu (2010). The details of this estimation procedure are discussed in Supplementary Data S.3.4.1.

3.4.2. Case study 1 by Dejong and Harris (1971)

Dejong and Harris (1971) reported the settlement of a 27-storey apartment building on dense clay till in Edmonton, Alberta, Canada. The settlement was monitored over a 6-year period. The 27-storey building was founded on 179 Franki expanded base piles which were approximately 0.60 m in diameter. These are high-capacity cast-in-place deep foundation piles constructed with a drop weight and

Please cite this article in press as: Hamderi, M., Comprehensive group pile settlement formula based on 3D finite element analyses, Soils Found. (2018), https://doi.org/10.1016/j.sandf.2017.11.012

Table 8
Soil parameters and geometrical values used in case studies.

1 No	2 fr (kN/m)	3 tr (kN)	4 No of Piles	5 No of Piles along x	6 No of Piles along y	7 Avg. sp_x (m)	8 Avg. sp_y (m)	9 le (m)	10 di (m)	11 wi_x (m)	14 wi_y (m)	13 bed (m)	14 th (m)
1	300	1000	179	23.7	7.5	2.7	2.7	4.9	0.60	60.4	17.4	25	0.60
2	205	683	132	13.3	9.9	2.7	2.7	7.6	0.41	33.5	24.3	24	0.50
3	425	1417	48	9.0	5.3	3.5	3.5	18.6	0.85	27.6	15.0	18	0.91
4	260	867	281	16.8	16.8	1.7	1.7	25.0	0.52	26.9	26.9	21	4.25
5	260	867	697	40.0	17.4	2.1	2.1	13.4	0.52	81.5	34.3	23	1.20

	15	16	17	18	19 settlement @centre			20 settlement @corner			21 deflection	
No	W.Avg. E1–E4 around Piles (MPa)	E5 (MPa)	ld (kPa)	Econc (MPa)	Case Study (m)	Formula (m)	Difference in %	Case Study (m)	Formula (m)	Difference in %	Case Study %	Formula %
1	99.5	180	246	25,000	**0.033**	**0.034**	**3.3%**	**0.015**	**0.013**	**15.9%**	**0.06%**	**0.07%**
2	8.8	44	131	25,000	**0.084**	**0.074**	**11.7%**	**0.035**	**0.035**	**0.4%**	**0.24%**	**0.19%**
3	63.0	130	256	25,000	**0.022**	**0.019**	**15.8%**	**0.018**	**0.010**	**43.2%**	**0.03%**	**0.05%**
4	18.4	70	254	25,000	**0.040**	**0.038**	**5.5%**	**N/A**	**0.025**	**N/A**	**N/A**	**N/A**
5	22.5	59	324	25,000	**0.200**	**0.166**	**16.9%**	**0.120**	**0.063**	**47.1%**	**0.18%**	**0.23%**
						Avg. Dev. →	**10.7%**		**Avg. Dev. →**	**26.7%**	**Avg. Dev. →**	**44.0%**

casing. This technique is a good choice for cohesionless soils such as sand and gravel. The thickness of the raft was not reported; therefore, it was assumed to be as thick as the diameter of the piles. The raft dimensions were approximately 17.4 m × 60.4 m. The final dead load of the building was 258.1 MN which is equivalent to a distributed load of 246 kPa.

The building was constructed on a soil profile, in descending order, of silty clay, dense sandy clay till (SPT-N_{60} ≈ 70 blow/ft), dense sand, gravel and finally about 30 m in depth of sandstone and mudstone. The soil profile and other details are summarized in Fig. 12. The set of soil moduli (E1, E2, E3, E4 and E5) required for the settlement estimation was interpolated from the elastic moduli estimated for each layer. The details of this estimation procedure are discussed in Supplementary Data S.3.4.2. For this case, the calculated settlements at the centre and at the corner resulted in 0.033 m and 0.013 m, respectively, which are in 3.3% and 15.9% proximity of the measured values, 0.034 m and 0.015 m, respectively. The details of the calculation, including the deflection rate, are given in Table 8.

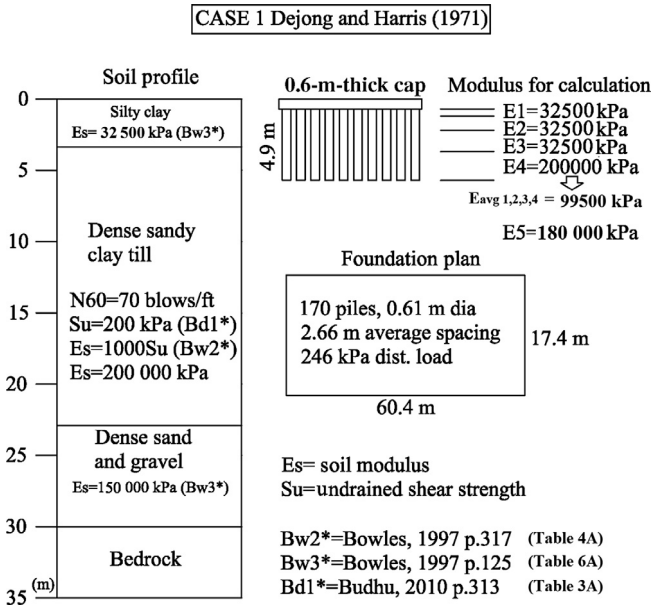

Fig. 12. Summary of parameters used for Case Study 1 by Dejong and Harris (1971).

3.4.3. Case study 2 by Koerner and Partos (1974)

Koerner and Partos (1974) reported the settlement of a 19-storey concrete building on a medium dense sand layer. The settlement was monitored over a 2-year period. The 19-storey building was founded on 132 pedestal-type piles (cast-in-situ) which were approximately 0.41 m in diameter. The expanded tip was about 0.76 m in diameter. The average thickness of the pile raft was not reported; therefore, a value of 0.5 m was assigned to the thickness. The foundation dimensions were approximately 24.3 m × 33.5 m. The final dead load of the building was 107 MN which is equivalent to a distributed load of 131 kPa. The building was constructed on a soil profile, in descending order, of fine sand, organic silt, poorly graded fine sand, well-graded sand, poorly graded fine sand and finally about 30 m of highly dense sand. The soil profile and other details are summarized in Fig. 13. The details of this estimation procedure are discussed in Supplementary Data S.3.4.3. The soil profile and other details are summarized in Fig. 13. For this case, the calculated settlements at the centre and at the corner resulted in 0.074 m and 0.035 m,

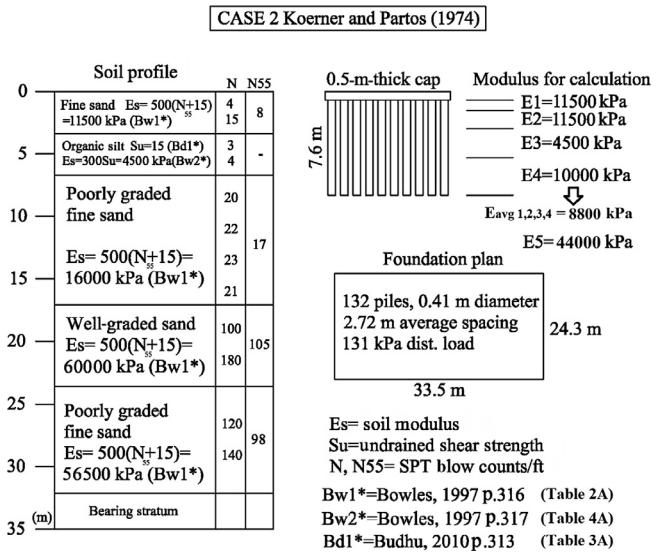

Fig. 13. Summary of parameters used for Case Study 2 by Koerner and Partos (1974).

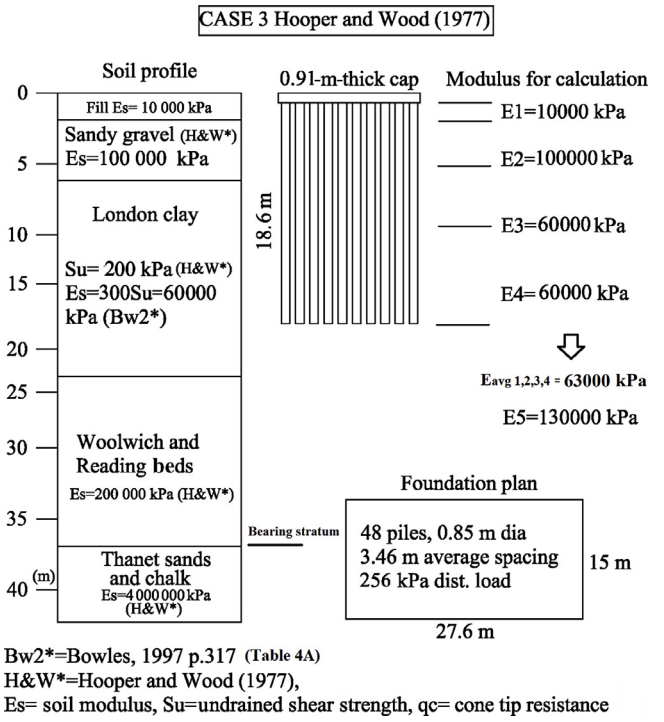

Fig. 14. Summary of parameters used for Case Study 3 by Hooper and Wood (1977).

respectively, which are in 11.7% and 0.4% proximity of the measured values, 0.084 m and 0.035 m, respectively.

3.4.4. Case study 3 by Hooper and Wood (1977)

Hooper and Wood (1977) reported the settlement of a 22-storey building on a medium dense sand layer. The settlement was monitored over a 5-year period. The 22-storey building was founded on 48 cast under-reamed piles with an average diameter of 0.85 m. The under-reamed piles are bored cast-in-situ piles which may contain one or more enlarged bulbs. The average thickness of the pile raft was 0.91 m. The foundation dimensions were approximately 15.0 m × 27.6 m. The final dead load of the building was 106 MN which is equivalent to a distributed load of 256 kPa. The building was constructed on a soil profile, in descending order, of fill, sandy gravel, London clay, Woolwich and Reading beds and Thanet sand and chalk. The soil profile and other details are summarized in Fig. 14. The details of this estimation procedure are discussed in Supplementary Data S.3.4.4. The soil profile and other details are summarized in Fig. 14. For this case, the calculated settlements at the centre and at the corner resulted in 0.019 m and 0.010 m, respectively, which are in 15.8% and 43.2% proximity of the measured values, 0.022 m and 0.018 m, respectively.

3.4.5. Case study 4 by Borsetto et al. (1991)

Borsetto et al. (1991) reported the settlement of a chimney 200 m in height and 11.6 m in bottom diameter located in a power plant complex in the Po Valley, Italy. The settlement was monitored over a 7-year period. The chimney was founded on a circular raft, 30.4 m in diameter and 4.25 m in thickness, and supported by 281 Franki piles, 0.52 m in diameter and 25 in length. The circular raft was incorporated in the calculations as a square raft with a side length of 26.9 m. The final dead load of the chimney was 184 MN which is equivalent to a distributed load of 254 kPa. The building was constructed on a soil profile, in descending order, of clayey silt, silt, sand and hard clayey silt layers. The soil profile and other details are summarized in Fig. 15. The details of this estimation procedure are discussed in Supplementary Data S.3.4.5. For this case, the calculated maximum vertical settlement resulted in 0.038 m which is in 5.5% proximity of the measured value, 0.040 m (Table 8). The settlement measured at the corner for this case was not reported; therefore, no comparison could be made for the corner settlement.

3.4.6. Case study 5 by Goossens and Van Impe (1991)

Goossens and Van Impe (1991) reported the settlement of 40 cylindrical reinforced concrete silos, 52 m in height and 8 m in diameter, founded on a rectangular area of 34.3 m × 85.1 m. The silos were built on a 1.2-m-thick foundation raft supported by 697 driven cast-in-situ reinforced concrete piles which were 13.4 m in length and 0.51 m in diameter.

The raft was split into three pieces with expansion joints along its longer side. The piles, which are located in Ghent, Belgium, had been driven into the ground in the early 1970s. It is reported that driven cast-in-situ piles were used mainly because of their cost-effectiveness. In order to manufacture these piles, a hallow tube is inserted into the ground. Subsequently, the hollow cylinder is filled with concrete for reinforcement. Finally, the hallow tube is pulled up and close contact between the concrete and the soil is achieved. The average load of a single pile was

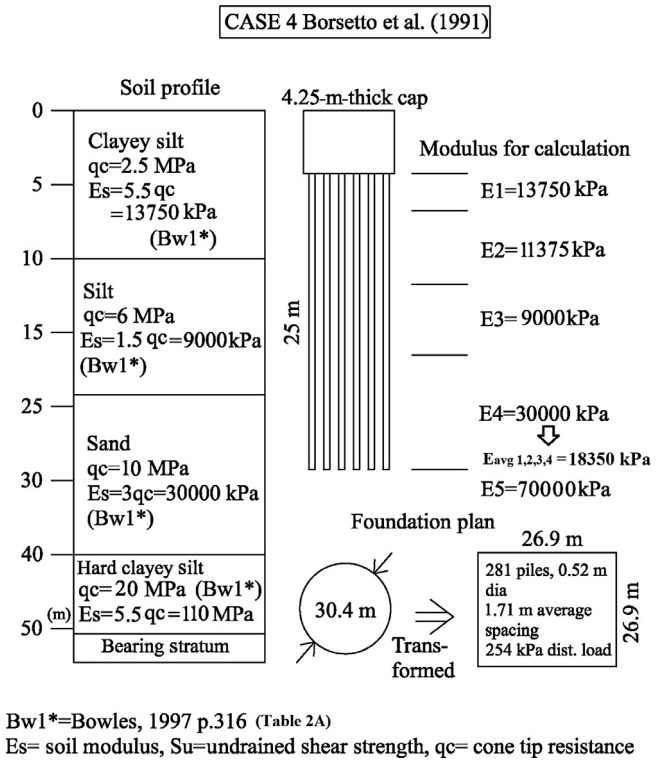

Fig. 15. Summary of parameters used for Case Study 4 by Borsetto et al. (1991).

reported as 1300 kN. It was also reported that the allowable loads became much greater than 2000 kN. A structure group weight of 906 MN acted on these piles and this was converted to a distributed load of 324 kPa.

The structure group was built on a soil profile, in descending order, of loamy or clayey sand, medium stiff clay, dense sand and finally tertiary clay. The soil profile and other details are summarized in Fig. 16. The details

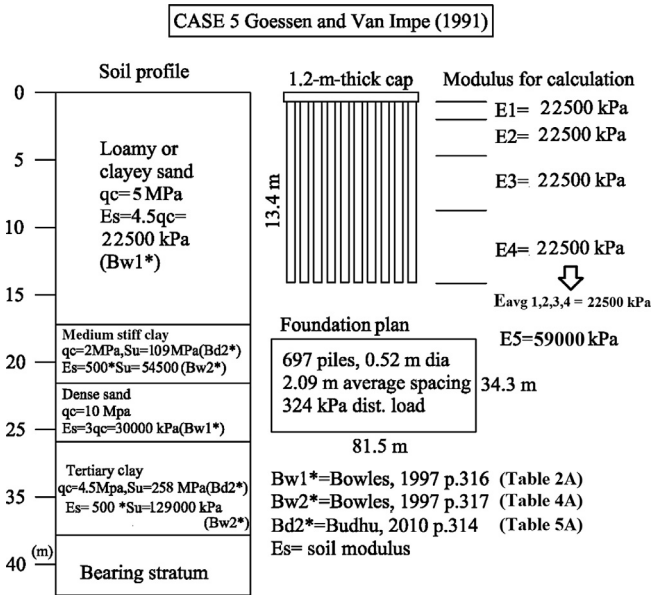

Fig. 16. Summary of parameters used for Case Study 5 by Goossens and Van Impe (1991).

of this estimation procedure are discussed in Supplementary Data S.3.4.6. The settlement was monitored over an 11-year period. During this period, a considerable amount of consolidation settlement occurred. For this case, the estimated settlements by the formula at the centre and at the corner were 0.166 m and 0.063 m, respectively, which are in 16.9% and 47.3% proximity of the measured values, 0.200 m and 0.120 m, respectively.

Although percentagewise a deviation of 16.9% is not considered to demonstrate a poor estimation, the absolute differences between the measured and the predicted results were considerably high compared to other cases. The formula miscalculated the settlement by about 34 mm at the centre of the raft. The relatively high deviation in the results is attributed to the long-term consolidation settlement mechanism which may be better estimated by formulas intended for consolidation settlement.

3.4.7. Identification of pile types to which the formula is applicable

In the last section, the estimation performance of the formula for the five case studies was seen to be quite high. The common trait of these cases was that they included cast-in-situ pile types in which the soil in the hole was removed before casting the piles. On the other hand, a different scenario is seen for the piles that are driven directly into the soil with heavy pile-driving equipment. In this case, as the pile is driven, the pile tip compresses the soil in front. Phuong et al. (2016) reports an increase in stress of about 100 times at the tip during the driving, an increase of 2.5 times in the pile bearing capacity and a decrease of 5% in the void ratio (=compaction) after the pile driving. In light of these findings, it can be said that in precast driven piles, there is great chance that the soil modulus of the surrounding soil will increase and this will lead to errors in the settlement estimation. Therefore, it is not recommended that the settlement formula be used for driving precast piles. The pile settlement formula is more applicable to cast-in-situ piles (cased or bored), where the inner soil is removed before the pile installation.

3.4.7.1. FE modelling of case 5 using split foundation. In Case 5, the foundation had three pieces which were separated by expansion joints. However, the formula used in the settlement calculation considered the foundation as one piece. In efforts to investigate the error associated with this simplification, further FE analyses were conducted. A discussion on this topic is included in Supplementary Data S.3.4.6.1.

3.4.8. Settlement analysis of case studies using equivalent pier method

In this section, the settlement of group piles will be calculated using the equivalent pier method offered by Poulos and Davids (1980) and Poulos (1993, 2001, 2006). In this method, the group pile system is replaced with a pier which has an equivalent diameter of d_e. The length (L) of the pier

is similar to that of the piles in the pile group. The equivalent diameter of the pier can be calculated from the following equation (Poulos, 1993, 2006):

$$d_e = (1.13\ to\ 1.27).(A_G)^{0.5} \quad (3)$$

where A_G = the plan area of the pile group, "1.13" is predominantly for end-bearing piles and "1.27" is for friction and floating piles. In the present case, an average value of "1.20" is incorporated. After calculating the equivalent diameter, the procedure is simplified to a problem of finding the settlement of a single pier. The settlement of a pier in a homogeneous soil can be calculated by the following formula (Poulos, 2001):

$$S = \frac{PI_s}{d_e E_s} \quad (4)$$

where P = is the total load acting on the pile group in kN, I_s = settlement coefficient and E_s = the average soil modulus around the piles. In order to find settlement coefficient I_s, the diagram illustrated in Fig. 17 can be used (Poulos, 2001). In addition to the above-mentioned parameters, the diagram also requires input parameters, such as pile length (L) and base soil modulus E_b. It should be noted that, the equivalent of E_s and E_b in the 3D FE-based formula is the weighted average of (E_1, E_2, E_3 and E_4) and E_5, respectively (Table 8, columns 15 and 16). The calculation flow is given stepwise in Table 9. In steps 1 to 3, equivalent diameter d_e is calculated using Eq. (3). In steps 4 to 9, settlement coefficient I_s is determined using the diagram given in Fig. 17. In step 11, the settlement is finally calculated using Eq. (4) (Poulos, 2001). The rest of the steps are devoted to comparing the settlement results with the measured values. The percent deviation in settlement is 20% when the formulas offered by Poulos (1993, 2001, 2006) (Eqs. (3) and (4)) are used. The same deviation is

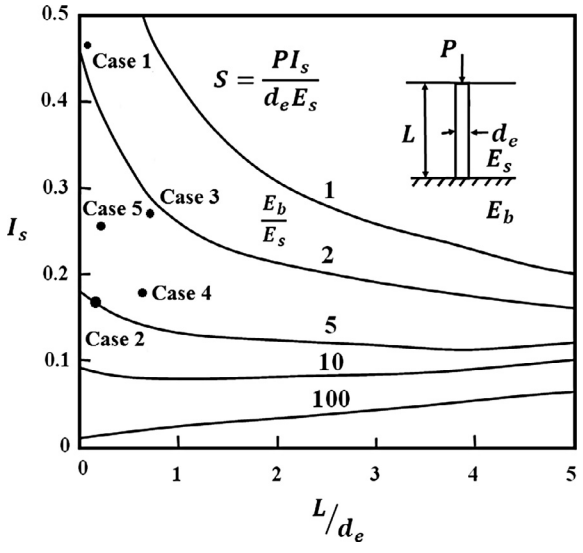

Fig. 17. Settlement calculation chart for equivalent pier method (reconstructed from Poulos, 2001).

Table 9
Calculation steps of equivalent pier method.

	1	2	3	4	5	6	7	8
Case No	A_G	D	d_e	L	L/de	E_s	E_b	E_b/E_s
-	m^2	M	m	m	-	MPa	MPa	-
1	1051	0.61	38.9	4.9	0.13	99.5	180	1.81
2	814	0.41	34.2	7.6	0.22	8.8	44	5.00
3	414	0.85	24.4	18.6	0.76	63.0	130	2.06
4	724	0.52	32.3	25.0	0.77	18.4	70	3.81
5	2795	0.52	63.4	13.4	0.21	22.5	59	2.62
		9	10	11	12	13	14	15
Case No		I_s	P	S_{Poulos}	S_{author}	$S_{measured}$	Dev_{Poulos}	Dev_{Author}
-		-	MN	m	m	m	%	%
1		0.46	259	0.031	0.034	0.033	7%	3%
2		0.18	107	0.064	0.074	0.085	25%	13%
3		0.28	106	0.019	0.019	0.022	12%	16%
4		0.18	184	0.056	0.038	0.040	40%	6%
5		0.26	906	0.165	0.166	0.200	18%	17%
						Avg. Dev.-->	20%	11%

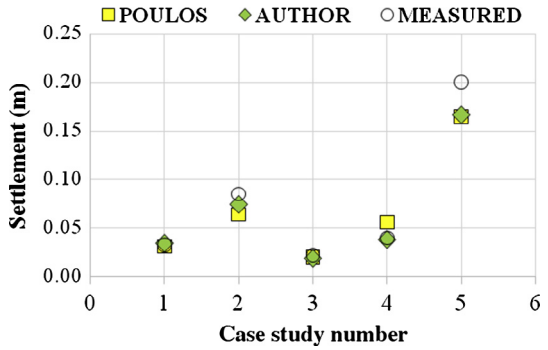

Fig. 18. Settlements obtained from three different sources.

11% by the formula offered in this study (Table 8). Looking at the settlement values obtained from each of the three sources, namely, Poulos (1993, 2001, 2006), the author and the measured ones (see Fig. 18), it can be seen that both approaches provide fairly close settlement results.

4. Physical meanings of input parameters of formula

If our settlement formula (Eq. (1)) is rewritten in the form of $S = S_b.x_1^{t1}\ldots x_{12}^{t12}$, exponents t1, t2, ..., t12 at first may look like they give a hint on how each (x_n) parameter is related to settlement S. For example, fitting coefficient "e" in the $\left(\frac{0.1E_1+0.2E_2+0.3E_3+0.4E_4+u_7}{u_8}\right)^e$ term is supposed to be "−1" at in the small strain range because the settlement and the soil modulus are inversely proportional, whereas this value is reported as "−0.4275" in Table 5. Such a disagreement between the expected and the estimated values may lead to the idea that there is a problem with the estimation. This would be a misleading judgement in our case because the disagreement between the expected and the

Please cite this article in press as: Hamderi, M., Comprehensive group pile settlement formula based on 3D finite element analyses, Soils Found. (2018), https://doi.org/10.1016/j.sandf.2017.11.012

Table 10
Base-line system and evaluation of pile length.

	1	2	3	4	5	6	7	8	9	10	11	12	13	14	15	16	17	18
1	Side Frict. (kN/m)	Max Tip Res. (kN)	Pile Spac. @x (m)	Pile Spac. @y (m)	Length of Pile (m)	Dia. of Pile (m)	Width of Max @x (m)	Width of Max @y (m)	Cap Thick. (m)	(0.1*E1 +0.2*E2 +0.3*E3 +0.4*E4)	E5	Load (kPa)	Ec (MPa)	Sett. by Formula @center (m)	Sett. by Formula @corner (m)	Norm. Pile Length	Norm. Sett.	Norm. Sett. Diff. (m)
2	300	1000	3.5	3.5	8	1	20	20	1	30000	30000	300	25000	0.106	0.080	0.40	1.40	1.26
3	300	1000	3.5	3.5	12	1	20	20	1	30000	30000	300	25000	0.092	0.069	0.60	1.22	1.15
4	300	1000	3.5	3.5	16	1	20	20	1	30000	30000	300	25000	0.083	0.061	0.80	1.09	1.07
5	300	1000	3.5	3.5	20	1	20	20	1	30000	30000	300	25000	0.076	0.055	1.00	1.00	1.00
6	300	1000	3.5	3.5	24	1	20	20	1	30000	30000	300	25000	0.070	0.050	1.20	0.92	0.94
7	300	1000	3.5	3.5	28	1	20	20	1	30000	30000	300	25000	0.065	0.046	1.40	0.85	0.89
8	300	1000	3.5	3.5	32	1	20	20	1	30000	30000	300	25000	0.060	0.042	1.60	0.79	0.84
9	300	1000	3.5	3.5	35	1	20	20	1	30000	30000	300	25000	0.056	0.039	1.75	0.74	0.80

estimated values is the consequence of the interaction of terms in the multi-variable formula. This interaction results in a shifting of the magnitudes of the exponential coefficients. For this reason, a special procedure is followed in this section to find the exponential relation of each individual input parameter on settlement. In this procedure, each time a certain parameter is targeted, the influences of the other parameters are filtered out. In this way, it is possible to see, for example, if coefficient "e" ends up being around "−1" when the influences of the other parameters are filtered out. As the first step of the evaluation procedure, a certain FE model configuration is designated as a base-line system. The input parameters of the base-line system are given in Table 10, row 5.

As the second step, some other combinations are derived by changing a certain input parameter each time. Subsequently, the settlement is calculated for these combinations. For example, Table 10 shows the pool of combinations which are used to plot the change in pile length versus settlement (Table 10, row 5 and columns 14–15). One further step is to normalize the settlement and input parameters with those of the base-line system (Table 10, columns 16–18). In this way, the input parameters vs. settlement plots will yield values around 1. For example, the plots in Fig. 19a demonstrate the change in pile length by means of the total and differential settlements, respectively.

If the trend curves in the form of $y = x^t$ are associated with these plots, the exponent values (t) become −0.43 and −0.31, respectively. From the mathematical point of view, the absolute value of "t" of function $y = x^t$ indicates how closely the x and y parameters are related. In other words, the greater the absolute t value, the stronger the relation. A schematic of the $y = x^t$ function is given for different signs of t in Fig. 19b. The positive sign for "t" indicates a direct relation between x and y, whereas a negative sign indicates an inverse relation. In this study, "t" will be

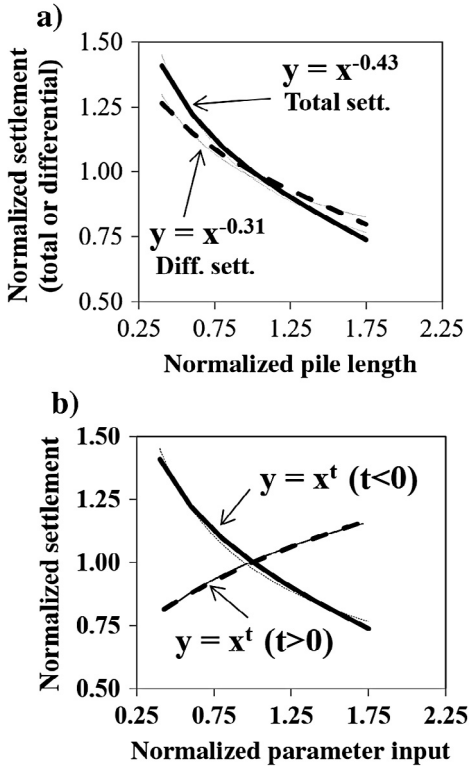

Fig. 19. (a) Variation in normalized settlement vs. normalized pile length and their trend curves, (b) General shape of normalized settlement vs. normalized input parameter curves.

called "the influence coefficient". The normalized settlement and normalized parameter input plots can generally be defined in the form of $y = x^t$.

The influence coefficients of all the input parameters for the total and differential settlement cases are given in Figs. 20 and 21, respectively. The input parameters that are directly and inversely related to settlement are given in blue and red colours, respectively.

Please cite this article in press as: Hamderi, M., Comprehensive group pile settlement formula based on 3D finite element analyses, Soils Found. (2018), https://doi.org/10.1016/j.sandf.2017.11.012

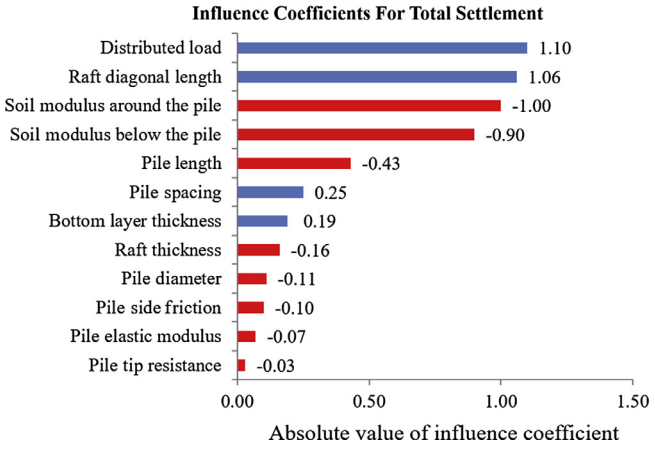

Fig. 20. Influence coefficients for total settlement.

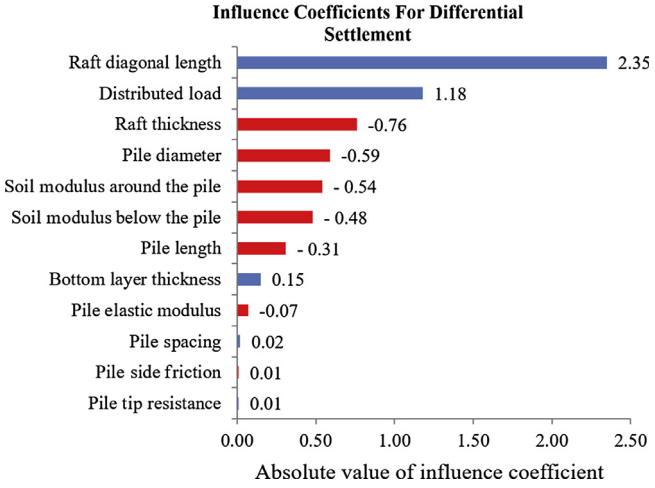

Fig. 21. Influence coefficients for differential settlement.

By reviewing Figs. 20 and 21, it can be said that input parameters, such as the distributed load and the raft diagonal length (for these cases, $|t| > 1$), are the most influential parameters in both types of settlement. It is also seen that the soil modulus has a great influence on the total settlement ($|t| > 0.9$), whereas it is less influential on the differential settlement ($|t| > 0.48$). It is interesting that the influence of the raft thickness is much greater on the differential settlement ($|t| = 0.76$) than on the total settlement ($|t| = 0.16$). In other words, it can be said that increasing the raft thickness, th (or the bending stiffness of the raft = EI = function of th = E.(width).th^3/12), is not very effective in reducing the total settlement, whereas it is quite helpful for reducing the differential settlement ($|t| = 0.76$).

One other interesting result is that the influence of the pile diameter on the total and differential settlement is quite different ($|t| = 0.11$ and $|t| = 0.59$, respectively). The influence of the pile diameter on the differential settlement is quite high, whereas the pile diameter is not very influential on the total settlement. It should be mentioned that the diameter of the pile here is only related to the axial stiffness. The skin friction which normally increases with an increasing diameter is defined as a separate input. In addition, the influence of the elastic modulus of the pile is relatively low ($|t| = 0.07$).

5. Conclusions

In this study, a comprehensive group pile settlement formula for the calculation of group pile settlement is presented. This formula incorporates the dimensions of a rectangular raft, namely, the diameter, length and spacing of the piles, vertical uniform pressure, soil moduli up to five layers, ultimate pile-soil friction, pile tip resistance and elastic modulus of the pile. The following conclusions can be drawn from the study:

- The formula includes all the main parameters that influence the settlement of group piles.
- The formula is 3D FE-based; therefore, the average prediction performance of the formula is considerably high based on the comparisons made with five real-case scenarios. In particular, the prediction performance was very high in the first four scenarios where the soil layers did not go under consolidation settlement. However, in the fifth case, the settlement prediction of the formula was less accurate due to consolidation.
- The raft settlements in five cases were also calculated by the equivalent pier method offered by Poulos (1993, 2001 and 2006). The results were in agreement with the measured values and also with the ones that were estimated by the 3D FE-based formula.
- An additional formula for the average raft deflection was offered. In this way, engineers can iterate through the input parameters until they find the most economical pile configuration for their structure.
- "An influence coefficient" term is introduced in order to demonstrate the rate of influence of each parameter in the formula. The most influential parameters become applied uniform load, soil modulus and the dimensions of the raft. On the other hand, the diameter, length and spacing of the piles have medium influence. The fact that piles are designed to resist at least two times their service load (usually a factor of safety > 2), there is always an extra skin resistance that is not activated within the pile or in the adjacent pile. Since, in group piles, an excessive load acting on a pile can easily be shared with the adjacent pile, the side friction and the tip resistance become less influential on the group pile settlement unlike what is normally observed in a single pile load test.

Acknowledgment

This study was supported by Turkish – German University Scientific Research Projects Commission under the grant no: 2018BM0004.

Please cite this article in press as: Hamderi, M., Comprehensive group pile settlement formula based on 3D finite element analyses, Soils Found. (2018), https://doi.org/10.1016/j.sandf.2017.11.012

Supplementary material

Supplementary data associated with this article can be found, in the online version, at https://doi.org/10.1016/j.sandf.2017.11.012.

References

ASTM D3080-3, 2013. Standard Test Method for Direct Shear Test of Soils under Consolidated Drained Conditions, ASTM International, West Conshohocken, PA.

Borsetto, M., Barbera, G., Colleselli, F., Colombo, P., Corti, G., Failella, D., Tripiciano, L., Giuseppett, G., Mazza, G., Varagnolo, P., 1991. Settlement analysis of main buildings in power plants by means of 2-D and 3-D models. In: Proceedings of the 10th European Conference on Soil Mechanics and Foundation Engineering, Florence, vol. 1, 323–328.

Bowles, J.E., 1997. Foundation Analysis and Design. 5th ed. McGraw-Hill Inc.

Budhu, M., 2010. Soil Mechanics and Foundations. 3rd ed. John Wiley & Sons Inc.

Chow, Y.K., 1986. Analysis of vertically loaded pile groups. Int. J. Numer. Anal. Meth. Geomech. 10 (1), 59–72.

Clancy, P., Randolph, M.F., 1996. Simple design tools for piled raft foundations. Geotechnique 46 (2), 313–328.

Cummings, A.E., Kerkhoff, G.O., Peck, R.B., 1950. Effect of driving piles in soft clay. Trans. ASCE 115, 275–286.

D'Appolonia, D.J., Lambe, T.W., 1971. Performance of four foundations on end-bearing piles. J.S.M.F.D., ASCE, vol. 97, SM I, 77–93.

DeJong, J., Harris, M.C., 1971. Settlement of two multi-story buildings in Edmonton. Can. Geotech. J. 8 (2), 217–235.

Diana User's Manual, 2014. Release 9.5, TNO DIANA BV, Netherlands.

Domone P., Illston J., 2010. Construction Materials-Their Nature and Behaviour. 4th ed. Spon Press.

Dung, N.T., Chung, S.G., Kim, S.R., 2010. Settlement of large-scale piled foundations using equivalent raft approach. ICE Proceedings Geotechnical Engineering, 163.

Fellenius, B.H., 1984. Negative skin friction and settlement of piles. In: Second International Seminar, Pile Foundations, Singapore, 12–24.

Fellenius, B.H., 1991. Pile Foundations. Foundation Engineering Handbook, 2nd ed. Chapman & Hall, New York, pp. 511–536.

Fellenius, B.H., 2006. Results from long-term measurement in piles of drag load and downdrag. Can. Geotech. J. 43 (4), 409–430.

Fellenius, B.H., Broms, B.B., 1969. Negative skin friction for long piles driven in clay. In: Proc. 7th Int. Conf. S.M. and. F.E., vol. 2, 93–98.

Goossens, D., Van Impe, W.F., 1991. Long term settlement of a pile group foundation in sand, overlaying a clayey layer. In: Proceedings of the 10th European Conference on Soil Mechanics and Foundation Engineering, Florence 1, 425–428.

Grimstad, G., Degago, S.A., Nordal, S., Karstunen, M., 2010. Modelling creep and rate effects in structured anisotropic soft clays. Acta Geotech. 5 (1), 69–81.

Hanna, T.H., 1967. The measurement of pore water pressures adjacent to a driven pile. Can. Geo. J. 4 (3), 313.

Housel, W.S., Burkey, J.R., 1948. Investigation to determine the driving characteristics of piles in soft clay. In: Proc. 2nd Int. Conf. S.M. & F. E., vol. 5, 146–154.

Hooper, J.A., Wood, L.A., 1977. Comparative behaviour of raft and piled foundations. In: Proceedings of the 9th International Conference on Soil Mechanics and Foundation Engineering, Tokyo, pp. 545–550.

Koerner, A.M., Partos, A., 1974. Settlement of building on pile foundation in sand. J. Soil Mech. Found. Div., ASCE 100 (3), 265–278.

Koizumi, Y., Ito, K., 1967. Field tests with regard to pile driving and bearing capacity of piled foundations. Soils Found. 3, 30.

Lambe, T.W., Horn. H.M., 1965. The influence on an adjacent building of pile driving for the M.I.T. materials centre. In: Proc. 6th Int. Conf. S. M. and F.E., vol. 2, p. 280.

Lo, K.Y., Stermac, A.G., 1965. Induced pore pressures during pile driving operations. In; Proc. 6th Int. Conf. S.M. and F.E., vol. 2, 285.

Meyerhof, G.G., 1976. Bearing capacity and settlement of pile foundations. J. Geotech. Eng., ASCE 102 (GT3), 195–228.

Orrje, O., Broms, B.B., 1967. Effects of pile driving on soil properties. J.S. M.F.D., ASCE, vol. 93, SM5, 5973.

Ottolini, M.G., Dijkstra, J., 2014. Novel surface speckle preparation method for imaging techniques for clay models. Géotechnique Lett. 4, 62–66.

Phuong, N.T.V., van Tol, A.F., Elkadi, A.S.K., Rohe, A., 2016. Modelling of pile installation using the material point method. Comput. Geotech. 73, 58–71.

Poulos, H.G., Davis, E.H., 1980. Pile Foundation Analysis and Design. Wiley & Sons, New York.

Plaxis 3D user's Manual (Software Version: AE: 01), 2013. Edited by Brinkgreve R.B.J., Engin E., Swolfs W.M., Delft, Plaxis BV.

Poulos, HG., 1993. Settlement prediction for bored pile groups. Proceedings of the 2nd Geotechnical Seminar on Deep Foundations on Bored and Auger Piles Ghent, 103–117.

Poulos, H.G., 2001. Geotechnical and Geoenvironmental Engineering Handbook, R.K. Rowe (Ed.). New York, pp. 278–279.

Poulos, H.G., 2006. Pile group settlement estimation – research to practice. Innovative Methods. GSP 153.

Poulos, H.G., Davis, E.H., 1980. Pile Foundation Analysis and Design. Wiley & Sons, New York.

Randolph, M.F., Wroth, C.P., 1979. An analysis of the vertical deformation of pile groups. Geotechnique 29 (4), 423–439.

Shahin, M., 2014. Load-settlement modeling of axially loaded steel driven piles using CPT-based recurrent neural networks. Soils Found. 54 (3), 515–522.

Sivasithamparam, N., Karstunen, M., Brinkgreve, R.B.J., Bonnier, P.G., 2013. Comparison of two anisotropic rate dependent models at element level. In: Proceedings of the International Conference on Installation Effects in Geotechnical Engineering, Rotterdam, the Netherlands, 23–27 March 2013.

Terzaghi, K., Peck, R.B., 1967. Soil Mechanics and Foundation Engineering Practice. Wiley, New York.

Yamashita, K., Tanikawa, T., Hamada, J., 2015. Applicability of simple method to piled raft analysis in comparison with field measurements. Geotech. Eng. J. SEAGS & AGSSEA 46 (2), 43–53.

Vesic, A.S., 1977. Design of pile foundations. National Cooperative Highway Research Program Synthesis of Practice No. 42. Transport Research Board, Washington, DC.

Von Wolffersdorff, P.A., 1996. A hypoplastic relation for granular materials with a predefined limit state surface. Mech. Cohesive-Frict. Mater. 1 (3), 251–271.

Zhu, G., Yin, J.H., 2000. Elastic visco-plastic consolidation modelling of clay foundation at Berthierville test embankment. Int. J. Numer. Anal. Meth. Geomech. 24 (5), 491–508.

Please cite this article in press as: Hamderi, M., Comprehensive group pile settlement formula based on 3D finite element analyses, Soils Found. (2018), https://doi.org/10.1016/j.sandf.2017.11.012